Generation of solitons by a boxlike pulse in the derivative nonlinear Schrödinger equation with nonvanishing boundary conditions

Volodymyr M. Lashkin*
Institute for Nuclear Research, Pr. Nauki 47, Kiev 03680, Ukraine
(Received 21 January 2005; revised manuscript received 28 April 2005; published 28 June 2005)

The creation of solitons of the derivative nonlinear Schrödinger equation with nonvanishing boundary conditions from a boxlike initial pulse is considered. The inverse scattering transform is used. An equation for soliton eigenvalues is obtained. It is shown that simultaneous generation of breathers (solitons with internal oscillations) and one-parametric (nonoscillating) bright or dark solitons is possible. For some sets of initial parameters only breathers or only one-parametric solitons emerge. No more than three bright solitons can emerge (possibly, simultaneously with breathers) in any case, while dark solitons or breathers can arise in arbitrary number when the corresponding thresholds are exceeded. Analytical estimates for the number of generated solitons and the corresponding thresholds are given in some particular cases.

DOI: 10.1103/PhysRevE.71.066613 PACS number(s): 05.45.Yv, 42.81.Dp

I. INTRODUCTION

The derivative nonlinear Schrödinger equation (DNLSE) ($\alpha=\pm 1$)

$$i\partial_t u + \partial_x^2 u + i\alpha\partial_x(|u|^2 u) = 0 \tag{1}$$

arises in two important physical areas—in space plasma physics and in nonlinear optics. First, Eq. (1) describes modulated small-amplitude nonlinear Alfvén waves in a low-β (the ratio of kinetic to magnetic pressure) plasma, propagating parallel [1–3] or at a small angle [4,5] to the ambient magnetic field. In this case $u=(B_y \pm iB_z)/B_0$ denotes the transverse magnetic field perturbation normalized by the ambient magnetic field B_0, where t and x are normalized time and space coordinates, respectively. The DNLS equation also describes large-amplitude magnetohydrodynamic waves in a high-β plasma, propagating at an arbitrary angle to the ambient magnetic field [6]. Second, the DNLS equation (1) is related to the modified nonlinear Schrödinger (MNLS) equation [where $\sigma=\pm 1$ corresponds to the abnormal (normal) group velocity dispersion (GVD) region]

$$i\partial_\tau\psi + \frac{\sigma}{2}\partial_\xi^2\psi + is\partial_\xi(|\psi|^2\psi) + |\psi|^2\psi = 0 \tag{2}$$

by a simple gaugelike transformation

$$\psi(\xi,\tau) = u(x,t)\exp\{(it)/(4s^4) + (i\sigma x)/(2s^2)\}, \tag{3}$$

where $\xi=(\sigma x)/(2s)+t/(2s^3)$ and $\tau=(\sigma t)/(2s^2)$. In turn, the MNLS equation describes the propagation of ultrashort femtosecond nonlinear pulses in optical fibers, when the spectral width of the pulses becomes comparable with the carrier frequency, and, in addition to the usual Kerr nonlinearity, the effect of self-steepening of the pulse should be taken into account [7]. In this case, $u(x,t)$ is the normalized slowly varying amplitude of the complex field envelope, t is the normalized propagation distance along the fiber, and x is the normalized time measured in a frame of reference moving with the pulse at the group velocity.

Equation (1) is completed by the boundary conditions: vanishing ($u\to 0$ as $|x|\to\infty$) or nonvanishing ($|u|\to\rho$ =const as $|x|\to\infty$) at infinity. In both cases the DNLSE is integrable by the inverse scattering transform (IST) [8,9], and admits N-soliton solutions [10]. The IST formalism for the DNLSE with nonvanishing boundary conditions is much more complicated than the one for vanishing boundary conditions. Analytical properties of the Jost solutions in this case are formulated on the Riemann sheets of the spectral parameter [9]. Recently, Chen and Lam [11] developed the IST for the DNLSE with nonvanishing boundary conditions by introducing an affine parameter to avoid constructing the Riemann sheets.

The nonvanishing boundary conditions are important in physical applications. For example, in space plasma physics the vanishing boundary conditions are relevant only for the case of propagation of Alfvén waves strictly parallel to the ambient magnetic field. In nonlinear optics the nonvanishing boundary conditions can support propagation of dark solitons in both normal and abnormal GVD regions [11].

The aim of this paper is to consider generation of solitons by a bounded boxlike initial profile in the DNLSE with nonvanishing boundary conditions. This task is one of the few for which the corresponding Cauchy problem allows an analytical consideration. Though analogous tasks for the nonlinear Schrödinger equation (NLSE) were solved long ago [12–15], we show that evolution of the rectangular initial pulses in the DNLSE with nonvanishing boundary conditions is highly nontrivial and significantly different from all known results. Unlike the NLSE or the DNLSE with vanishing boundary conditions, one-soliton solution of the DNLSE with nonvanishing boundary conditions represents a breather (oscillating soliton) [11]. The "usual" (i.e., nonoscillating) solitons correspond to degenerate breathers, when the real part of the one-soliton eigenvalue is zero. We show that nonoscillating solitons and breathers can arise simultaneously. For some sets of initial parameters only breathers or only the usual solitons (bright or dark) emerge. The dynam-

*Electronic address: vlashkin@kinr.kiev.ua

ics of soliton generation strongly depends on parameters of the initial boxlike profile and the background, and it turns out to be quite interesting. For example, we demonstrate that no more than three bright usual solitons can emerge in any case, while dark solitons or breathers can arise in arbitrary number.

Without loss of generality, we will consider the nonvanishing boundary conditions in the form

$$u \to \rho \exp(\pm 2i\theta) \quad \text{as } x \to \pm\infty. \tag{4}$$

We also put $\alpha=1$, since the case $\alpha=-1$ can be obtained from the former by a transformation $x \to -x$.

The paper is organized as follows. In Sec. II we give necessary information about spectral problems associated with the DNLSE with nonvanishing boundary conditions. Tnen, equations for the Jost solutions for the case of an arbitrary initial bounded profile are derived, and the scattering coefficients are presented in terms of these Jost solutions. A boxlike initial profile is considerd in Sec. III, and an explicit equation determining the discrete spectrum of the spectral problem is obtained. Then, some particular cases are investigated in more detail. The conclusion is made in Sec. IV.

II. BASIC EQUATIONS

According to Ref. [8] the direct scattering problem corresponding to Eq. (1) is

$$\frac{\partial \varphi_1}{\partial x} = -i\lambda^2 \varphi_1 + \lambda u \varphi_2,$$

$$\frac{\partial \varphi_2}{\partial x} = -\lambda u^* \varphi_1 + i\lambda^2 \varphi_2, \tag{5}$$

where λ is a spectral parameter. The asymptotics of the Jost solutions of the spectral problem (5) with the boundary conditions (4) are [11]

$$\Phi \to e^{-i\theta\sigma_3} \begin{pmatrix} 1 \\ -\dfrac{i\rho}{\zeta} \end{pmatrix} e^{-ik(\zeta)x} \quad \text{as } x \to -\infty, \tag{6}$$

$$\Phi \to e^{i\theta\sigma_3} \begin{pmatrix} a(\zeta)e^{-ikx} - b(\zeta)\dfrac{i\rho}{\zeta}e^{ikx} \\ b(\zeta)e^{ikx} - a(\zeta)\dfrac{i\rho}{\zeta}e^{-ikx} \end{pmatrix} \quad \text{as } x \to \infty, \tag{7}$$

where an affine parameter ζ and the function $k(\zeta)$ have been introduced by the relations

$$\lambda = \frac{1}{2}\left(\zeta - \frac{\rho^2}{\zeta}\right), \quad k(\zeta) = \frac{1}{2}\left(\zeta + \frac{\rho^2}{\zeta}\right)\lambda(\zeta). \tag{8}$$

In Eqs. (6) and (7), $\Phi=(\varphi_1,\varphi_2)^{\mathrm{T}}$ and $a(\zeta)$ and $b(\zeta)$ are the scattering coefficients.

A generic initial profile will reshape itself into a set of N solitons and continuous radiation (quasilinear modes). The latter always disperses away and decays, while the solitons will propagate as coherent units. Solitons correspond to the discrete spectrum of the problem (5). The number of emerging solitons N is equal to the number of zeros $\zeta_n=\rho\exp(\gamma_n+i\beta_n)$ of the coefficient $a(\zeta)$ with $\gamma_n \geq 0$, $0<\beta_n<\pi/2$, where $n=1, 2, \ldots$. The parameters γ_n and β_n represent the parameters of the nth soliton. The corresponding one-soliton solution Eq. (A1) is given in the Appendix. In the general case, when $\gamma_n \neq 0$, the soliton is usually called a two-parametric soliton. It represents a soliton with internal oscillations (a breather). When $\gamma_n \to 0$, there is only one parameter β_n characterizing the soliton, and it is called a one-parametric soliton. The one-parametric solution is presented by Eq. (A8). There are two types of one-parametric solitons, bright and dark. In bright solitons $|u|>\rho$, while in dark solitons $|u|<\rho$.

Let us consider the case when the initial profile u is different from background only in some finite region in x, so that at $t=0$ we have

$$u(x,0) = \begin{cases} \rho e^{-2i\theta}, & -\infty < x < 0, \\ u_0(x), & 0 \leq x \leq l, \\ \rho e^{2i\theta}, & l < x < \infty. \end{cases} \tag{9}$$

Note that such a profile is quite natural from the practical point of view, since, in reality, input optical pulses always have finite duration. For Alfvén waves in magnetized plasma, the profile (9) represents an initial tangential discontinuity of the magnetic field perturbation, which is a typical situation for nonlinear plasma magnetohydrodynamics [16]. In a space plasma, magnetic holes and magnetic decreases bounded by tangential discontinuities were observed experimentally [17].

The continuity conditions for $\Phi(x)$ at $x=0$ and l yield, respectively,

$$\Phi(0,\zeta) = e^{-i\theta\sigma_3} \begin{pmatrix} 1 \\ -\dfrac{i\rho}{\zeta} \end{pmatrix}, \tag{10}$$

$$\Phi(l,\zeta) = e^{i\theta\sigma_3} \begin{pmatrix} ae^{-ikl} - b\dfrac{i\rho}{\zeta}e^{ikl} \\ be^{ikl} - a\dfrac{i\rho}{\zeta}e^{-ikl} \end{pmatrix}. \tag{11}$$

Now the scattering coefficients depend on the parameter l. From Eqs. (5) one can obtain the following equation:

$$\frac{d^2\varphi_1}{dl^2} - \frac{u'_0}{u_0}\frac{d\varphi_1}{dl} + \lambda^2\left(|u_0|^2 - i\frac{u'_0}{u_0} + \lambda^2\right)\varphi_1 = 0, \tag{12}$$

where $u_0=u_0(l)$, $u'_0=du_0/dl$. Equation (12) is completed by the "initial" (at $l=0$) conditions

$$\varphi_1(l=0,\zeta) = e^{-i\theta}, \tag{13}$$

$$\left.\frac{d\varphi_1(l,\zeta)}{dl}\right|_{l=0} = -i\lambda^2 e^{-i\theta} - i\lambda u_0 \frac{\rho}{\zeta} e^{i\theta}, \tag{14}$$

which follow from Eqs. (5) and (10). The equation for $\varphi_2(l)$ is obtained by complex conjugation of Eq. (12). The corresponding initial conditions are

$$\varphi_2(l=0,\zeta) = -\frac{i\rho}{\zeta}e^{i\theta}, \tag{15}$$

$$\left.\frac{d\varphi_2(l,\zeta)}{dl}\right|_{l=0} = -\lambda u_0^* e^{-i\theta} + \lambda^2\frac{\rho}{\zeta}e^{i\theta}. \tag{16}$$

As follows from Eq. (11), the coefficient $a(\zeta)$ is connected with $\varphi_1(l,\zeta)$ and $\varphi_2(l,\zeta)$ by the relation

$$a(\zeta)\left(1+\frac{\rho^2}{\zeta^2}\right)e^{-ik(\zeta)l} = \varphi_1(l,\zeta)e^{-i\theta} + \frac{i\rho}{\zeta}\varphi_2(l,\zeta)e^{i\theta}. \tag{17}$$

Having determined $\varphi_1(l,\zeta)$ and $\varphi_2(l,\zeta)$ from Eqs. (12)–(16), one can get an equation determining the zeros of $a(\zeta)$ (i.e., the soliton eigenvalues).

III. BOXLIKE PROFILE

Analytical solutions of Eqs. (12)–(16) are possible only in a few simple cases. Consider the case of a boxlike profile, i.e., when $u_0(x)=u_0\exp(iq)$, where u_0 is a constant real amplitude and q is a constant phase. In this case the equations for φ_1 and φ_2 can be easily solved. The solutions are

$$\varphi_1(l,\zeta) = e^{-i\theta}\cos(Bl) - i\lambda\left(\lambda e^{-i\theta} + u_0\frac{\rho}{\zeta}e^{i\theta+iq}\right)\frac{\sin(Bl)}{B}, \tag{18}$$

$$\varphi_2(l,\zeta) = -\frac{i\rho}{\zeta}e^{i\theta}\cos(Bl) + \lambda\left(\lambda\frac{\rho}{\zeta}e^{i\theta} - u_0 e^{-i\theta-iq}\right)\frac{\sin(Bl)}{B}, \tag{19}$$

where $B=\lambda\sqrt{u_0^2+\lambda^2}$. Therefore, as follows from Eq. (17), the zeros of $a(\zeta)$ are determined from the equation

$$\frac{\lambda[\lambda(\rho^2e^{2i\theta} - \zeta^2e^{-2i\theta}) - 2u_0\rho\zeta\cos q]}{i(\rho^2e^{2i\theta} + \zeta^2e^{-2i\theta})}\tan(Bl) = B. \tag{20}$$

Solitons correspond to the roots $\zeta_n=\rho\exp(\gamma_n+i\beta_n)$ with $\gamma_n\geqslant 0$, $0<\beta_n<\pi/2$. Denoting $\eta=\gamma+i\beta$ and introducing the variables $r=\rho l^{1/2}$, $s=u_0l^{1/2}$, one can rewrite Eq. (20) in the form

$$\frac{\tan D}{D} = \frac{i\cosh(2i\theta-\eta)}{r\sinh\eta[r\sinh\eta\sinh(2i\theta-\eta) - s\cos q]}, \tag{21}$$

where

$$D = r\sinh\eta\sqrt{r^2\sinh^2\eta + s^2}. \tag{22}$$

In the asymptotics $t\to\infty$ the field $u(x,t)$ will represent a set of solitons with the parameters (γ_n,β_n). In the general case, when $\gamma_n\neq 0$, the soliton with the parameters γ_n and β_n is actually a breather (oscillating soliton) with period

$$T_n = \frac{2\pi}{\rho^2\tanh(2\gamma_n)[\cosh^2(2\gamma_n) + \cos^2(2\beta_n)]} \tag{23}$$

and velocity

$$v_n = 2\rho^2 - \rho^2\cos(2\beta_n)\frac{\cosh(4\gamma_n)}{\cosh(2\gamma_n)}. \tag{24}$$

A. Phase jump

As the first example let us consider the simplest case when $l=0$, i.e., the initial profile is

$$u(x,0) = \begin{cases}\rho e^{-2i\theta}, & -\infty<x<0,\\ \rho e^{2i\theta}, & 0<x<\infty.\end{cases} \tag{25}$$

In this case we have just a phase step on a constant background. Then, as follows from Eq. (20), the equation determining the zeros of $a(\zeta)$ is

$$\rho^2e^{2i\theta} + \zeta^2e^{-2i\theta} = 0. \tag{26}$$

Having solved Eq. (26), one can see that there is only one soliton with the parameters

$$\gamma_1 = 0, \quad \beta_1 = 2\theta + \pi/2, \tag{27}$$

provided that $2\theta<0$. The velocity of the soliton is

$$v_1 = 2\rho^2 + \rho^2\cos(4\theta). \tag{28}$$

No soliton appears if $2\theta>0$.

The soliton with parameters (27) is the one-parametric soliton described by Eq. (A8). The question arises: What kind of soliton, bright or dark, emerges in our case? Since $|u(x,0)|^2-\rho^2=0$, this problem is not quite trivial. According to Eq. (A8), we should determine $\epsilon=\mathrm{sgn}(\sin\varphi_0)$. The case $\epsilon=-1$ (1) corresponds to a bright (dark) soliton. The parameters x_0 and φ_0 of the nth soliton (in our case $n=1$) can be found [11] from the coefficient

$$c_n(0) = \frac{b_n(0)}{\dot{a}(\zeta_n)} \tag{29}$$

where $\dot{a}(\zeta)=\partial a/\partial\zeta$ and $b_n(0)$ is the coefficient of proportionality between the two fundamental solutions of Eq. (5) evaluated at $\zeta=\zeta_n$ and $t=0$,

$$\Phi(x,\zeta_n,0) = b_n(0)\Psi(x,\zeta_n,0), \tag{30}$$

where $\Phi(x,\zeta)$ is the Jost solution with the asymptotics Eqs. (6) and (7), and the second fundamental solution $\Psi(x,\zeta)=(\psi_1,\psi_2)^T$ has the asymptotics [11]

$$\Psi \to e^{i\theta\sigma_3}\begin{pmatrix}-\dfrac{i\rho}{\zeta}\\ 1\end{pmatrix}e^{ik(\zeta)x} \quad \text{as } x\to\infty, \tag{31}$$

$$\Psi \to e^{-i\theta\sigma_3}\begin{pmatrix}-b^*(\zeta)e^{-ikx} - a(\zeta)\dfrac{i\rho}{\zeta}e^{ikx}\\ a(\zeta)e^{ikx} + b^*(\zeta)\dfrac{i\rho}{\zeta}e^{-ikx}\end{pmatrix} \quad \text{as } x\to-\infty. \tag{32}$$

The coefficient $c_1(0)$ is connected with x_0 and φ_0 by the relation

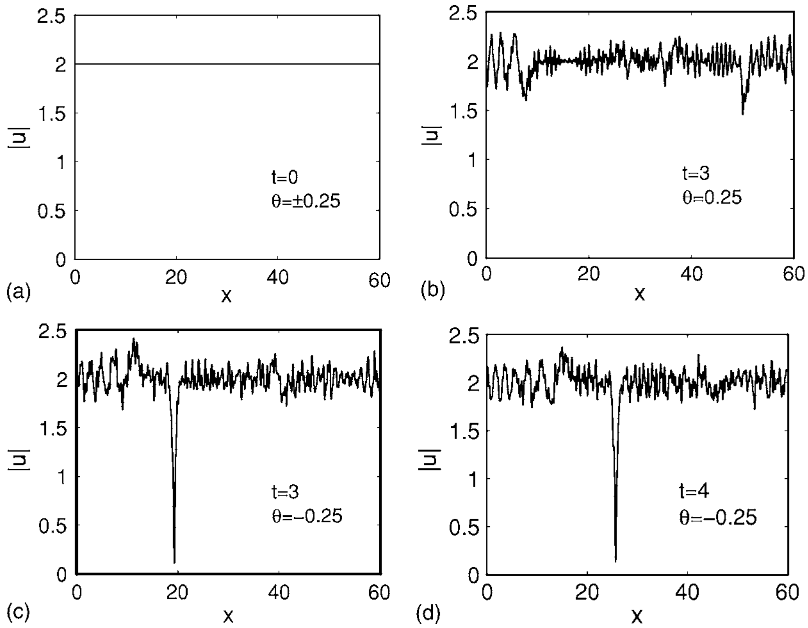

FIG. 1. Numerical solution of Eq. (1) for the initial profile Eq. (25) at $\rho=2$ and $\theta=\pm 0.25$. (a) Initial state at $t=0$. (b) The solution at time $t=3$ for the positive phase $\theta=0.25$. No soliton appears. (c) and (d) Dark soliton solution at $t=3$ and 4, respectively. The phase $\theta=-0.25$ is negative.

$$c_1(0) = \frac{2k(\zeta_1)}{i\zeta_1^*}\sin(2\beta_1)e^{\nu x_0 + i\varphi_0}. \quad (33)$$

As follows from Eqs. (6), (7), (25), (31), and (32) exact explicit expressions for the Jost solutions and the coefficient $a(\zeta)$ are

$$\Phi = \begin{pmatrix} e^{-i\theta} \\ -\dfrac{i\rho}{\zeta}e^{i\theta} \end{pmatrix}, \quad \Psi = \begin{pmatrix} -\dfrac{i\rho}{\zeta}e^{i\theta} \\ e^{-i\theta} \end{pmatrix}, \quad (34)$$

and

$$a(\zeta) = \frac{e^{-2i\theta} + (\rho^2/\zeta^2)e^{2i\theta}}{1 + \rho^2/\zeta^2}. \quad (35)$$

From Eqs. (29), (30), and (35) one can get $b_1(0)=-1$ and $c_1(0)=i\rho(1-\cos 4\theta)$. Comparing the latter expression with Eq. (33) we have $\varphi_0=-2\theta$, where $-\pi/2<2\theta<0$, and therefore

$$\epsilon = \mathrm{sgn}(\sin\varphi_0) = 1. \quad (36)$$

Thus, the dark soliton emerges.

Figure 1 shows the results of numerical solution of Eq. (1) for the initial condition given by Eq. (25) with $\rho=2$ and $\theta=\pm 0.25$. The simulations were performed in a box of length $L=60$. The function $U=u\exp(-4i\theta x/L)$ is periodic in this box and periodic boundary conditions were imposed on U. Spatial discretization was based on the pseudospectral method [18]. Temporal discretization included the implicit Crank-Nicholson scheme. Spectral resolution was 1024 including the dealiased modes. One can see that, in accordance with the analysis presented above, solitons do not emerge if the phase θ is positive, $\theta>0$. On the other hand, the only dark soliton appears if $\theta<0$. The velocity of the soliton, estimated from Figs. 1(c) and 1(d), is in good agreement with the analytical prediction Eq. (28).

B. Black box

Second, we consider the case when the initial field is absent in a region of length l, i.e., $u_0=0$ $(s=0)$. Then Eq. (21) takes the form

$$\tan(r^2\sinh^2\eta)\tanh(2i\theta-\eta) = i. \quad (37)$$

Separating the real and imaginary parts in Eq. (37), one can show that $\gamma=0$ and the parameter β is determined from the equation

$$\pi(n+1/2) + 2\theta = \beta_n + r^2\sin^2\beta_n, \quad (38)$$

where $n=0, 1, 2 \ldots$. Hence, only one-parametric solitons can be generated. Since $|u(x,0)|^2-\rho^2<0$, these solitons are the dark ones. The parameter β_n determines the amplitude of the nth soliton [see Eq. (A8)]. One can see that the solitons exist if

$$-\pi/2 < \pi n + 2\theta < r^2. \quad (39)$$

As follows from Eq. (38), the number N of emerging solitons is

$$N = \left[\frac{r^2 - 2\theta}{\pi}\right] + 1, \quad (40)$$

where [ ] means the integer part. One sees that at least one soliton always arises if $r^2>2\theta$. If the condition

$$r^2 \gg \pi(n+1/2) + 2\theta \quad (41)$$

is met, one can get the following analytical estimate for the parameter β_n:

$$\beta_n = \frac{\sqrt{1 + 4r^2[\pi(n+1/2) + 2\theta]} - 1}{2r^2}. \quad (42)$$

The condition (41) means that Eq. (42) is valid for considering the lowest eigenvalues with $n \ll N$. Under this we have $\beta_n \ll 1$.

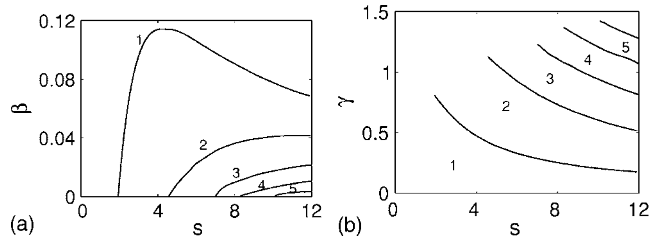

FIG. 2. The dependence of the soliton eigenvalues $\eta_n=\gamma_n+i\beta_n$ on s for $r=0.7$, $\theta=\pi/8$, $q=2$. The five first roots $n=1,\ldots,5$ are shown. In (a), the parameter β_n is plotted. In (b), the corresponding γ_n is plotted. Only breathers are generated for this set of parameters.

C. General case

The parameter β is connected with the amplitude of the soliton, and setting $\beta=0$ in Eq. (21), we get for the threshold value of γ (provided that $\gamma\neq 0$)

$$\gamma_{\text{th}}=\operatorname{arcsinh}\left(-\frac{s}{r}\cos 2\theta\cos q\right)^{1/2}. \tag{43}$$

This means, in particular, that two-parametric solitons are possible only if $\cos q<0$. The dependence of the soliton eigenvalues $\eta_n=\gamma_n+i\beta_n$, obtained from numerical solution of Eq. (20), on s for $r=0.7$, $\theta=\pi/8$ (note that $\sin 2\theta>0$), $q=2$ is presented in Fig. 2. The five first roots $n=1,\ldots,5$ are shown. Only breathers (since all roots have $\gamma\neq 0$) are generated for this set of parameters. Results of direct nuumerical simulations of the original Eq. (1) for the boxlike initial condition with the same parameters as in Fig. 2 and several different values of s are presented in Fig. 3. The simulations were performed in a box of length $L=80$. The numerical solutions are shown for time $t=4$. One can see that the number of emerging solitons is in full agreement with the results presented in Fig. 2. For example, no soliton appears if $s=1$ [Fig. 3(a)], and two solitons emerge [Fig. 3(c)] if $s=6$ (these solitons correspond to the roots numbered 1 and 2 in Fig. 2).

Since Eq. (21) is a transcendental equation with complex coefficients, it is reasonable to expect that, as a rule, its roots have nonzero real part. This corresponds to two-parametric (breather) soliton generation. We show below that one-parametric solitons can also be generated in a sufficiently wide range of input parameters. Setting $\gamma=0$ in Eq. (21) and denoting $z=\sin\beta$, we can write (provided that $\sin\beta\neq 0$) an equation determining the parameter β for one-parametric solitons in the form

$$F(z)=G(z), \tag{44}$$

where we have introduced the functions

$$F(z)=\frac{\tanh(rz\sqrt{s^2-r^2z^2})}{\sqrt{s^2-r^2z^2}(z\sin 2\theta+\cos 2\theta\sqrt{1-z^2})} \tag{45}$$

and

$$G(z)=-\frac{1}{rz(\sin 2\theta\sqrt{1-z^2}-z\cos 2\theta)+s\cos q} \tag{46}$$

with $0<z<1$. Consider some cases separately.

1. Case I

This is the case

$$s^2>r^2,\quad \sin 2\theta<0. \tag{47}$$

First we assume

$$r^2\sin^2 2\theta+2rs\cos q\cos 2\theta<4r^2s^2\cos^2 q, \tag{48}$$

so that $G(z)$ has no singularity on $[0;1]$. In this case, as one can show, the function $G(z)$ has one minimum at $z_{\min}=\cos\theta$. Under this,

$$G(0)=-\frac{1}{s\cos q},\quad G(1)=-\frac{1}{(s\cos q-r\cos 2\theta)}. \tag{49}$$

On the other hand, the function $F(z)$ monotonically increases from $z=0$ to $z_s=\cos 2\theta$, has a singularity at $z=z_s$, and monotonically increases from $z=z_s$ to $z=1$. Under this,

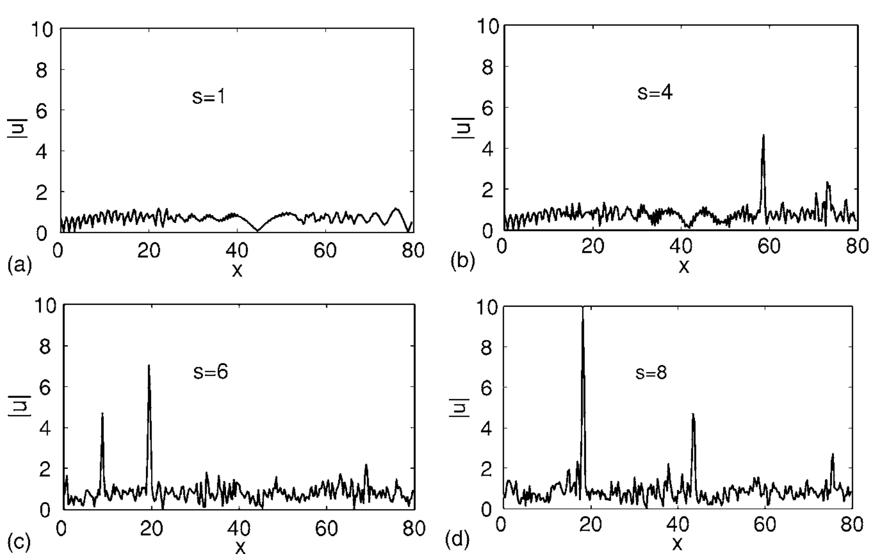

FIG. 3. Numerical solution of Eq. (1) at time $t=4$ for boxlike initial state with parameters $r=0.7$, $\theta=\pi/8$, $q=2$ (the same as in Fig. 2) and different values of s. (a) No solitons. (b) One soliton. (c) Two solitons. (d) Three solitons.

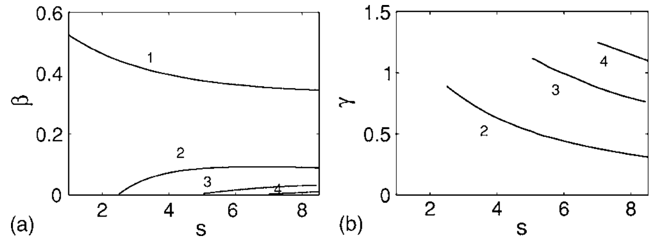

FIG. 4. The dependence of the soliton eigenvalues $\eta_n = \gamma_n + i\beta_n$ on s for $r=0.7$, $\theta=-\pi/8$, $q=2$. The four first roots $n=1,\ldots,4$ are shown. In (a), the parameter β_n is plotted. In (b), the corresponding γ_n is plotted; root numbered 1 has $\gamma=0$ (and corresponds to a one-parametric soliton).

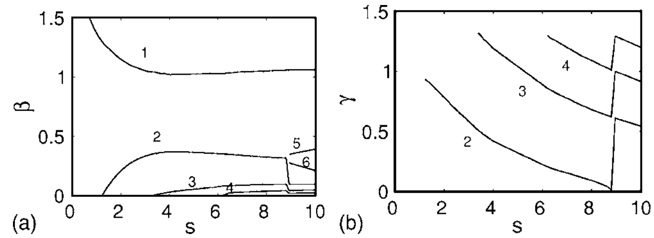

FIG. 5. The dependence of the soliton eigenvalues $\eta_n = \gamma_n + i\beta_n$ on s for $r=0.7$, $\theta=\pi/8$, $q=2.8$. The six first roots $n=1,\ldots,6$ are shown. In (a), the parameter β_n is plotted. In (b), the corresponding γ_n is plotted; roots numbered 1, 5, and 6 have $\gamma=0$ (and correspond to one-parametric solitons).

$$F(0) = 0, \quad F(1) = \frac{\tanh(r\sqrt{s^2 - r^2})}{\sin 2\theta\sqrt{s^2 - r^2}} < 0. \tag{50}$$

Taking into account that $z_{\min} > z_s$, and comparing the graphics of $F(z)$ and $G(z)$, one can see that there is one root β_1 of Eq. (44) if $\cos q < 0$. Under this, $\beta_1 < 2\theta$. If $\cos q > 0$, there is one root $\beta_1 > 2\theta$ if $F(1) \geqslant G(1)$, and there are two roots β_1 and β_2 if $F(1) < G(1)$. If the inequality (48) is violated, the function $G(z)$ has a singularity. A straightforward analysis shows that in this case Eq. (44) has only one root for both $\cos q < 0$ and $\cos q > 0$. As was said above, two-parametric solitons are possible only if $\cos q < 0$. Thus, if conditions (47) and $\cos q > 0$ are met, one or two bright (since $s > r$) one-parametric solitons emerge. If $\cos q < 0$, then, generally speaking, aside from the one bright soliton, which always arises, breathers can be generated. The number of breathers (possibly, zero) and the corresponding eigenvalues depends on s, r, θ, and q and can be found from Eq. (21) only numerically. The dependence of the soliton eigenvalues $\eta_n = \gamma_n + i\beta_n$ on s for $r=0.7$, $\theta=-\pi/8$, $q=2$ is presented in Fig. 4. The four first roots $n=1,\ldots,4$ are shown. The root numbered 1 corresponds to the one-parametric soliton. The other roots correspond to breathers. The number of breathers increases with increasing parameter s.

2. Case II

This is the case

$$s^2 > r^2, \quad \sin 2\theta > 0. \tag{51}$$

As in case I we first assume that condition (48) holds. Then the function $G(z)$ has one maximum at $z_{\max} = \sin\theta$ and

$$G(z_{\max}) = -\frac{1}{r\sin^2\theta + s\cos q}. \tag{52}$$

Boundary values of $G(z)$ are given by Eq. (49). The function $F(z)$ has no singularities and $F(z) > 0$. One can immediately conclude that if $G(z_{\max}) < 0$ and the condition (48) is met, there are two possibilities: only breathers are generated if $\cos q < 0$ (this case is presented in Fig. 1) and no solitons appears if $\cos q > 0$. A tedious but straightforward analysis shows that the function $F(z)$ can have no more than two extrema on $[0;1]$. Therefore, no more than three one-parametric solitons can be generated in the case Eq. (51). This result remains unchanged if the condition (48) is violated, and the function $G(z)$ has a singularity. This situation is presented in Fig. 5, where the dependence of the soliton eigenvalues $\eta_n = \gamma_n + i\beta_n$ on s is shown for $r=0.7$, $\theta=\pi/8$, and $q=2.8$. The six first roots $n=1,\ldots,6$ are shown. The roots numbered 1, 5, and 6 correspond to one-parametric solitons. The other roots correspond to breathers.

3. Case III

This is the case

$$s^2 < r^2. \tag{53}$$

The behavior of the function $G(z)$ for $\sin 2\theta < 0$ and $\sin 2\theta > 0$ is the same as in the cases I and II, respectively. The function $F(z)$ has tangentlike singularities. As one can see from Eq. (45), the number n_{sing} of the singularities is

$$n_{\text{sing}} = \left[\frac{r^2\sqrt{1 - s^2/r^2} - \pi/2}{\pi}\right], \tag{54}$$

where [ ] means the integer part. Since $G(z)$ has on $[0;1]$ either one extremum or one singularity, the number of roots of Eq. (44), N, is no less then n_{sing}. On the other hand, an analysis similar to that made above shows that $N \leqslant n_{\text{sing}} + 3$. Thus, the number of emerging one-parametric dark (since $s < r$) solitons N satisfies

$$n_{\text{sing}} \leqslant N \leqslant n_{\text{sing}} + 3. \tag{55}$$

Note that Eq. (55) with $s=0$ is in agreement with Eq. (40). Simultaneously breathers can emerge if $\cos q < 0$. Unlike cases I and II, an arbitrary number of one-parametric solitons arises if the corresponding threshold conditions are met. The dependence of $z_n = \sin\beta_n$ on the parameter s/r for $r=5$, $\theta = \pi/8$, and $q=1$ is presented in Fig. 6. Since $\cos q > 0$, only one-parametric solitons are generated. No more than eight dark solitons are possible for this set of parameters. The number of solitons for the given s/r is in accordance with Eq. (55) and can be estimated as $n_{\text{sing}} + 1$.

D. Initial pulse consisting of several boxes

In this subsection we describe how to obtain an equation determining soliton eigenvalues in the case when the initial profile consists of several, say M, separately located boxes.

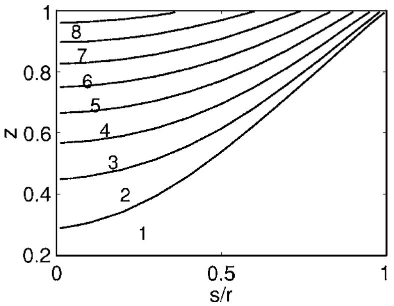

FIG. 6. The dependence of soliton eigenvalues $z_n=\sin\beta_n$ ($n=1,\ldots,8$) on s/r for $r=5$, $\theta=\pi/8$, $q=1$. Only one-parametric solitons are generated in this case.

Let each of the boxes be characterized by $u_{0,j}$, the phase q_j, and the pair (x_{2j-1},x_{2j}), where x_{2j-1} and x_{2j} are the start and the end points of the jth box, respectively ($j=1,\ldots,M$), so that $l_j=x_{2j}-x_{2j-1}$ is the length of the jth box, and let $x_1<x_2<x_3<\ldots<x_{2M}$. Then it is necessary to calculate the coefficients $a_j(\zeta)$ and $b_j(\zeta)$ of the monodromy matrix

$$S_j=\begin{pmatrix} a_j & -b_j^* \\ b_j & a_j^* \end{pmatrix} \tag{56}$$

separately for each of the boxes. An equation for $b_j(\zeta)$ can be obtained from Eq. (11) in the same way as an equation for $a_j(\zeta)$. Under this, the initial conditions Eqs. (13)–(16) are slightly modified, and the coefficients $a_j(\zeta)$ and $b_j(\zeta)$ depend on x_{2j-1} and x_{2j} (we had $x_1=0$, $x_2=l$). The resulting monodromy matrix (for all boxes), from which one can extract the coefficient $a(\zeta)$ that we need, is just the product (ordered) of these separate monodromy matrices:

$$S=\prod_{j=1}^{M} S_j. \tag{57}$$

Then, the equation for soliton eigenvalues is $a(\zeta)=0$.

IV. CONCLUSION

In this paper we have studied the possibility of soliton generation by a boxlike initial pulse for the derivative nonlinear Schrödinger equation with nonvanishing boundary conditions. Generation of two types of solitons is possible: breathers (two-parametric solitons) and one-parametric solitons (bright or dark). Equations for Jost solutions and an expression for the transmission coefficient $a(\zeta)$, determining the soliton eigenvalues, were derived for bounded initial profiles of arbitrary form. An explicit equation for the soliton eigenvalues was obtained in the case of a boxlike initial condition. We have shown that, generally speaking, the creation of solitons takes place without a threshold with respect to the area under the initial intensity profile. An even phase step on a constant background results in only the one-parametric dark soliton emerging, if the phase decreases (no solitons appear in the opposite case). In the general case, simultaneous generation of breathers and one-parametric solitons is possible. For some sets of initial parameters only breathers or only the usual solitons (bright or dark) emerge. For example, no breathers can be generated if the phase q of the initial profile satisfies $\cos q>0$. Similarly, in the case of the absence of an initial field (black box) it was shown that only one-parametric dark solitons can emerge, and depending on the background parameters the number of emerging solitons was determined (one can say that in this case the solitons are generated only by the background). The dynamics of soliton generation strongly depends on the parameters of the initial boxlike profile and the background, and it turns out to be quite nontrivial. For example, it was demonstrated that no more than three bright solitons can emerge in any case, while dark solitons can arise in arbitrary number.

The results obtained in this paper can be directly applied to Alfvén solitons in magnetized plasma [1–6], or, after the gaugelike transformation Eq. (3) of the initial condition [see Eq. (2)], to ultrashort femtosecond nonlinear pulses in optical fibers [7].

APPENDIX ONE-SOLITON SOLUTION

The one-soliton solution of Eq. (1) (with $\alpha=1$) for boundary conditions Eq. (4) is [11]

$$u(x,t)=\rho\frac{AB}{(B^*)^2}, \tag{A1}$$

where

$$A=\sinh 2\gamma_1\cosh(z+2\gamma_1+3i\beta_1-\ln\sinh 2\gamma_1) + \sin 2\beta_1\sinh(3\gamma_1-i\varphi), \tag{A2}$$

$$B=\sinh 2\gamma_1\cosh(z+2\gamma_1-i\beta_1-\ln\sinh 2\gamma_1) - \sin 2\beta_1\sinh(\gamma_1+i\varphi), \tag{A3}$$

with

$$z=\nu(x-vt-x_0),\quad \varphi=\mu(x-wt)+\varphi_0, \tag{A4}$$

$$\mu=\rho^2\sinh 2\gamma_1\cos 2\beta_1,\quad \nu=\rho^2\cosh 2\gamma_1\sin 2\beta_1, \tag{A5}$$

$$v=2\rho^2-\rho^2\cos 2\beta_1\frac{\cosh 4\gamma_1}{\cosh 2\gamma_1}, \tag{A6}$$

$$w=2\rho^2-\rho^2\cosh 2\gamma_1\frac{\cos 4\beta_1}{\cos 2\beta_1}. \tag{A7}$$

If $\gamma_1\to 0$ and $\varphi_0\neq n\pi$ (n is an integer), from Eq. (A1) we get the one-parametric soliton solution

$$u(x,t)=\rho\left[1-\frac{2\epsilon\cos^2\beta_1}{\sinh(z+i\beta_1)+\epsilon}\right], \tag{A8}$$

where x_0 has been redefined by absorbing $\ln[2\sin(2\beta_1)|\sin\varphi_0|]/\nu$ into x_0, and $\epsilon=\mathrm{sgn}(\sin\varphi_0)$. The case $\epsilon=-1$ (1) corresponds to the bright (dark) soliton.

[1] A. Rogister, Phys. Fluids **14**, 2733 (1971).
[2] E. Mjølhus, J. Plasma Phys. **16**, 321 (1976).
[3] K. Mio, T. Ogino, K. Minami and S. Takeda, J. Phys. Soc. Jpn. **41**, 265 (1976).
[4] E. Mjølhus, Phys. Scr. **40**, 227 (1989).
[5] C. F. Kennel, B. Buti, T. Hada, and R. Pellat, Phys. Fluids **31**, 1949 (1988).
[6] M. S. Ruderman, J. Plasma Phys. **67**, 271 (2002).
[7] Yu. S. Kivshar and G. P. Agraval, *Optical Solitons: From Fibers to Photonic Crystals* (Academic Press, San Diego, 2003).
[8] D. J. Kaup and A. C. Newell, J. Math. Phys. **19**, 798 (1978).
[9] T. Kawata and H. Inoue, J. Phys. Soc. Jpn. **44**, 1968 (1978).
[10] H. Steudel, J. Phys. A **36**, 1931 (2003).
[11] X.-J. Chen and W. K. Lam, Phys. Rev. E **69**, 066604 (2004).
[12] S. V. Manakov, Zh. Eksp. Teor. Fiz. **65**, 1392 (1973) [Sov. Phys. JETP **38**, 693 (1974)].
[13] D. J. Kaup, Phys. Rev. A **16**, 704 (1977).
[14] Yu. S. Kivshar, J. Phys. A **22**, 337 (1989).
[15] S. A. Gredeskul, Yu. S. Kivshar, and M. V. Yanovskaya, Phys. Rev. A **41**, 3994 (1990).
[16] A. I. Akhiezer, I. A. Akhiezer, R. V. Polovin, A. G. Sitenko, and K. N. Stepanov, *Plasma Electrodynamics* (Pergamon Press, Oxford, 1975).
[17] F. Verheest and G. S. Lakhina, Phys. Scr., T **98**, 38 (2002).
[18] J. P. Boyd, *Chebyshev and Fourier Spectral Methods* (Dover Publications, New York, 2000).